Influence of shear and bond on rotational capacity of reinforced concrete beams

Autor(en): **Bachmann, Hugo**

Objekttyp: **Article**

Zeitschrift: **IABSE publications = Mémoires AIPC = IVBH Abhandlungen**

Band (Jahr): **30 (1970)**

PDF erstellt am: **26.05.2024**

Persistenter Link: https://doi.org/10.5169/seals-23589

Influence of Shear and Bond on Rotational Capacity of Reinforced Concrete Beams

L'influence de la sollicitation de cisaillement et de l'adhérence des armatures sur la capacité de rotation des poutres en béton armé

Der Einfluß von Schubbeanspruchung und Verbund auf die Rotationsfähigkeit plastischer Stahlbeton-Gelenke

HUGO BACHMANN

Dr. sc. techn., Assistant Professor of Civil Engineering, Swiss Federal Institute of Technology, Zurich, Switzerland

Introduction

A considerable amount of experimental and theoretical research into the plastic behaviour of statically indeterminate structures has been carried out during the last 20 years. The application of the simple plastic analysis to steel structures has been shown to be valid. In statically indeterminate reinforced concrete structures, however, the rotational capacity of plastic hinges may be very small and as a result theoretical ultimate load can not be reached.

Since 1963 a research programme to study the influence of shear and bond on the general development and the rotational capacity of reinforced concrete plastic hinges has been carried out at the Institute of Structural Engineering of the Swiss Federal Institute of Technology (ETH), Zurich, Switzerland.

Test Specimens

The test series consisted of two groups of 5 symmetrical two-span beams, Series A of a rectangular cross section and Series B of an I-shaped cross section. The load arrangement and dimensions are shown in Fig. 1. The two end reactions were measured with dynamometers at every load step. Thus the value of the moment and shear at every cross section of the beams could be calculated from the equilibrium conditions.

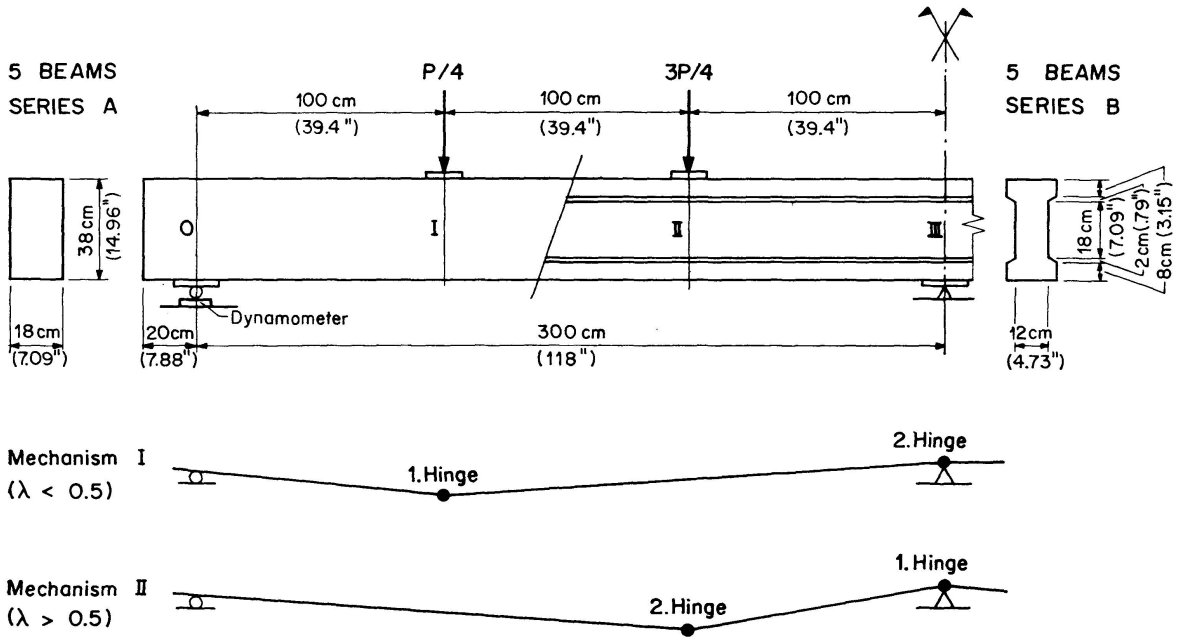

Fig. 1. Loading arrangement and dimensions of test specimens; mechanisms arrived at by plastic analysis.

The test beams were designed on a simple plastic analysis theory as given for instance in [1]. The ratio of the calculated ultimate moments in the spans and over the central support is denoted by λ. The value of λ determines where the first hinge is formed. The corresponding mechanisms are shown in Fig. 1. If $\lambda < 0.5$, Mechanisms I occurs, and if $\lambda > 0.5$, Mechanism II. $\lambda_e = 0.456$ corresponds to the elastic moment distribution. The plastic rotation necessary to allow the calculated ultimate load to be reached increases with the difference between λ and λ_e.

The values of λ for the 10 beams varied from 0.17 to 2.32. The longitudinal tensile reinforcement p varied from 0.34 to 2.04 percent in span and from 0.78 to 2.04 percent over the central support.

For the design of the shear reinforcement it was assumed that

$$V_c = v_c b' d \text{ with } v_c = 4 + 0.025 f'_c \text{ (kg/cm}^2\text{)} \quad (1)$$
$$(v_c = 57 + 0.025 f'_c \text{ [psi]})$$

is carried by the concrete compression zone. The stirrup reinforcement was calculated according to the truss analogy with a shear force of $V_u - V_c$ and a steel stress of f_y. The ultimate shear force V_u was calculated by the simple plastic analysis method.

An example of the stress-strain curve for the longitudinal and stirrup reinforcement (Torstahl) is shown in Fig. 2. The elastic limit stress f_e varied from 3200 to 3800 kg/cm^2 (nom. 46 to 54 ksi), the yield strength f_y (0.2 percent proof stress) from 3600 to 4800 kg/cm^2 (nom. 63 to 87 ksi). Good bond conditions were provided by a combination of spiral and non-continuous ribs. The

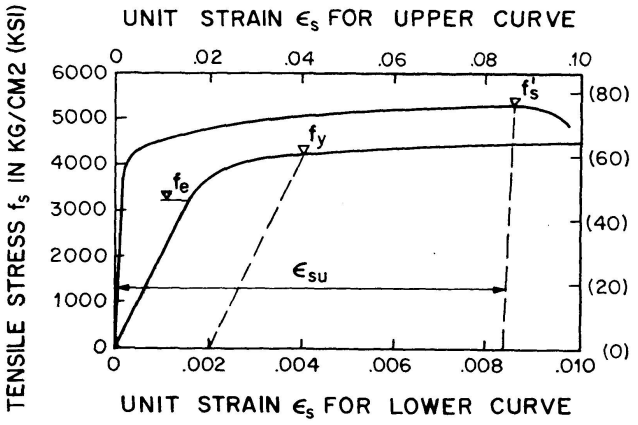

Fig. 2. Example of stress-strain curve of reinforcement.

average compressive strength of the concrete f'_c was 356 kg/cm² (nom. 5000 psi).

Tests to study rotational capacity are often carried out on simply supported one-span beams. However, with this test arrangement the following conditions could be investigated:

— At hinges in the spans: A small shear stress (but no pure bending!).
— At hinges over the central support: A high shear stress and a small moment-shear ratio ($M/Vd = 1.0 + 2.8$ due to contraflexure).
— At hinges in the spans and over the central support: A variation of the shear stress during rotation.

Test Results

In particular curvatures, rotations and the extensions of the stirrups were measured with dials and mechanical extensometers placed along the length of the beams.

General Behavior and Failure

In all the beams the mechanisms developed as predicted by the simple plastic analysis. In the beams A 1 and A 2 the first plastic hinge was formed in span, corresponding to Mechanism I, and in the other beams the first plastic hinge occured over the central support, corresponding to Mechanism II.

In 8 beams the collapse load reached or exceeded the ultimate load computed by the plastic analysis using a bilinear moment-curvature relationship. In 2 beams, however, the rotational capacity of the support hinge was not sufficient to enable the theoretical ultimate load to be reached.

3 beams (A 1, A 2, A 3) failed in span due to bending. The tensile reinforcement was elongated until the steel was ruptured. In the other 7 beams a shear failure occurred at the support hinge during plastic rotation. As the

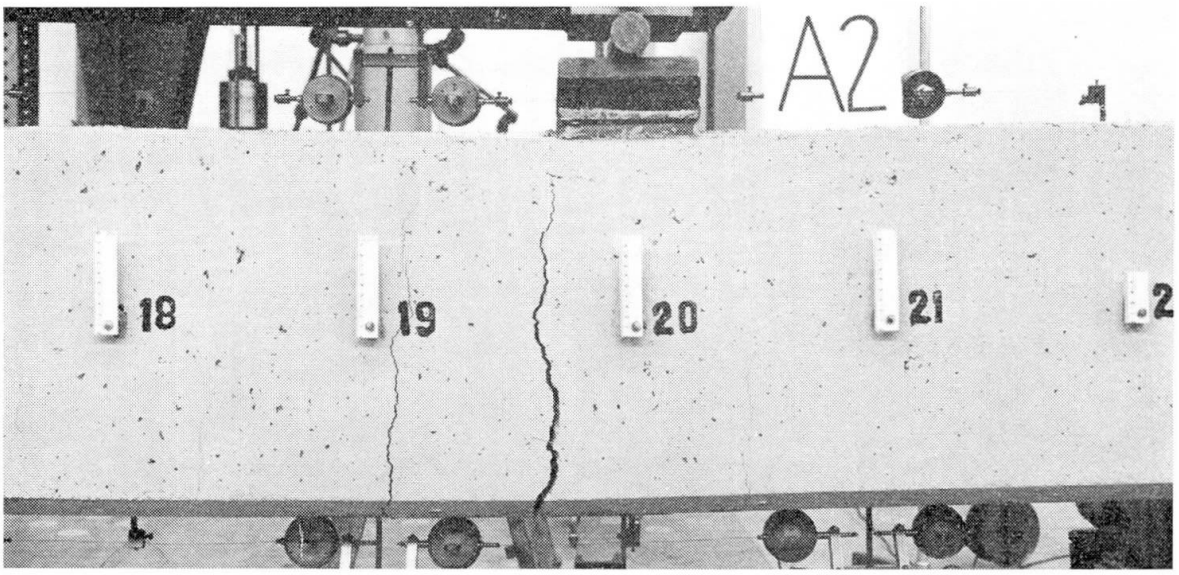

Fig. 3. Typical "flexural crack hinge", beam A 2.

stirrups deformed plastically, that is as their stress exceeded the elastic limit stress f_e, greater shear deformations in the web could be observed. These deformations caused high local stresses in the concrete of the web and the compression zone. Mainly as a result of these stirrup deformations the concrete in the web and the compression zone finally was crushed.

Plastic Hinges

Two entirely different types of plastic hinges were observed. They are described as

"flexural crack hinges", and
"shear crack hinges".

A typical flexural crack hinge is shown in Fig. 3. This type of hinge develops in a beam zone in which the bending moment is predominant. The shear stress is small and therefore only vertical flexural cracks occur. As seen in Fig. 3 plastic deformations were concentrated mainly to one crack. For this reason, the rotational capacity of such a flexural crack hinge may be very small.

A typical shear crack hinge behaves in another way (see Fig. 3). Diagonal flexural-shear cracks are produced through the influence of a relatively large shear stress in addition to the bending moment. This improves the behaviour of the hinge. The tests have shown that the plastic deformations in a shear crack hinge occur over a much wider zone than with flexural crack hinges, and this allows a much greater rotational capacity.

Rotational Behaviour

Plots of the moment ratio against the total rotation of the two types of plastic hinges as shown in Fig. 3 and 4 are given as examples in Fig. 5. The

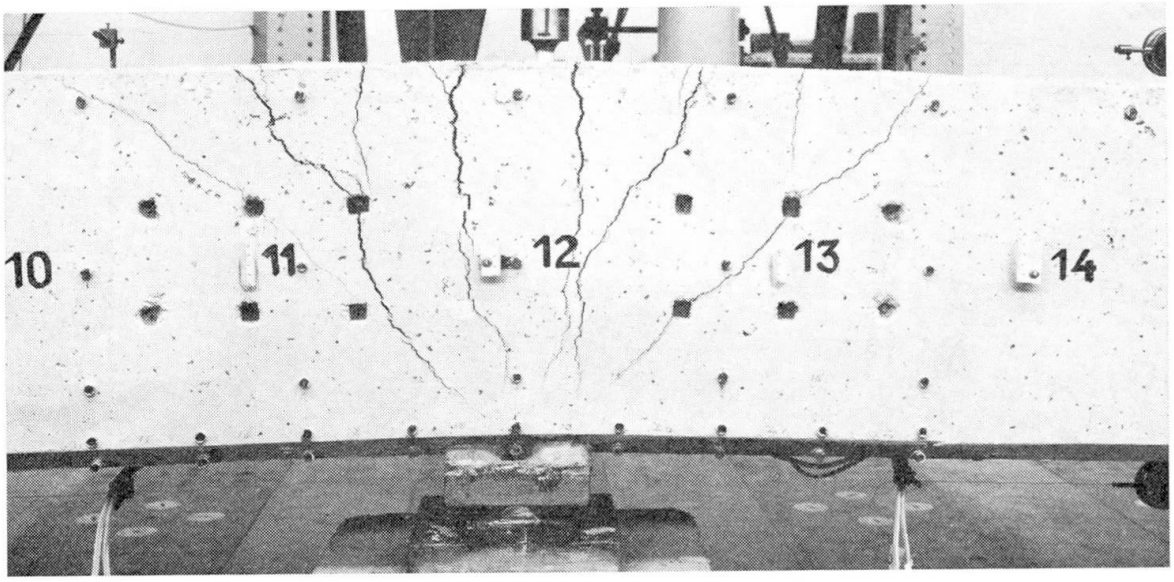

Fig. 4. Typical "shear crack hinge", beam A 5.

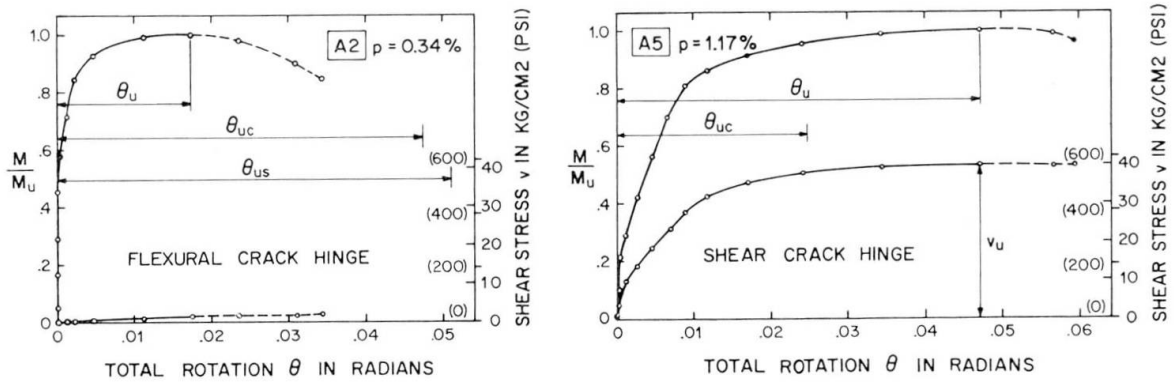

Fig. 5. Moment-rotation and shear stress-rotation relationship of a flexural crack hinge and of a shear crack hinge.

deformation of the hinges was considered to occur in the zone of plastic extension of the tensile reinforcement. This "plastic length L_p" was observed to be 25 cm (nom. 10 in.) at the flexural crack hinge of beam A 2 and 80 cm (nom. 31 in.) at the shear crack hinge of beam A 5. Also the nominal shear stress $v = V/b' d$ in the hinge is plotted against the total rotation in Fig. 5.

The rotational capacity can be characterized by the rotation θ_u which is reached at the ultimate moment M_u. Fig. 5 shows that the rotational capacity θ_u of the shear crack hinge is considerably greater than that of the flexural crack hinge. This result and the rupture of the tension steel in the span hinges of the beams A 1, A 2 and A 3 are incompatible with the usual view and theories as stated in [2] and [3] for instance.

Table 1 lists the values of the amount of the tensile reinforcement as a percentage p, the nominal shear stress v_u at M_u, and the corresponding moment-shear ratio $M_u/V_u d$ at the flexural crack hinge of the beams A 1, A 2, and A 3.

Table 1. Details, Measured and Calculated Values of Test Beams

Beam No.	p percent	v_u kg/cm² (psi)	$\frac{M_u}{V_u d}$	θ_u radians	θ_{uc} radians	$\frac{\theta_u}{\theta_{uc}}$	θ_{us} radians	$\frac{\theta_u}{\theta_{us}}$	θ_{ut} radians	$\frac{\theta_u}{\theta_{ut}}$
A 1	0.34	2.86 (41)	4.4	0.0100	0.0506	0.20	0.0477	0.21	0.0074	1.35
A 2	0.34	1.51 (21)	9.6	0.0173	0.0474	0.36	0.0509	0.34	0.0094	1.84
A 3	0.51	0.27 (4)	83	0.0188	0.0316	0.59	0.0525	0.36	0.0131	1.43

In addition, the rotations θ_u measured over a gauge length of 25 cm (nom. 10 in.) which included the zone of the steel rupture, are listed in Table 1. In beam A 2 plastic deformations of the steel were only produced within this gauge length. Plastic deformations could also be observed outside this gauge length in beam A 1 to a small extent and in beam A 3 to a greater extent. For this reason, the values of θ_u for A 1 and A 3 are only representative of the rotational capacity of the gauge length.

The values of θ_{uc} listed in Table 1 were calculated by the method given in [2] and [3]. θ_{uc} is computed by multiplying a "curvature of rupture" by the plastic length:

$$\theta_{uc} = \frac{\epsilon_{cu}}{c_0} L_p . \tag{2}$$

Taking into account the effect of the binding of the concrete compression zone by stirrups and compression steel as given in [3] the maximum concrete compressive strain ϵ_{cu} was found to be 0.0038. The depth of the neutral axis c_0 was computed neglecting the compression steel as given in ACI 318-63. The plastic length L_p was taken as the gauge length of θ_u, i. e. $L_p = 25$ cm (nom. 10 in.). Comparing θ_u and θ_{uc} in Table 1 it is found that the measured values reach to only 20 to 59 percent of the calculated values.

In analogy to Eq. (2) the total rotation θ_{us} for failure due to rupture of the tension steel is usually calculated by the following formula:

$$\theta_{us} = \frac{\epsilon_{s\,max}}{d - c_0} L_p , \tag{3}$$

in which ϵ_{max} means the maximum steel strain at rupture, viz:

$$\epsilon_{s\,max} = \epsilon_{su} + \frac{f'_s}{E_s} . \tag{4}$$

ϵ_{su} denotes the permanent steel strain measured on a gauge length not including the rupture zone (see Fig. 2). E_s is the modulus of elasticity of the steel.

For the calculation of θ_{us}, L_p was taken again as 25 cm (nom. 10 in.). The results listed in Table 1 show that θ_{us}, as well as θ_{uc}, considerably overrates the measured rotation θ_u. If θ_u, θ_{uc}, and θ_{us} were to be calculated with respect to the observed plastic length and the theoretical plastic length as given in [2] and [3], still greater differences would be obtained.

The situation is quite different with shear crack hinges. As an example the calculated rotation θ_{uc} of the beam A 5 is given in Fig. 5. It demonstrates that for shear crack hinges, θ_{uc} considerably underrates the measured rotation θ_u.

Shear Behaviour

In the cracked sections of flexural crack hinges the shear is almost exclusively carried by the concrete compression zone. If the stress in the tensile reinforcement exceeds the yield strength, any possible shear carrying capacity by interlocking of the aggregates is lost; nor is the dowel action of the tensile reinforcement usually significant.

It was of great interest to realize that in shear crack hinges the stirrup stress is not influenced by the hinge rotation. As an example the shear force V_c in the beam B 4 is plotted against the rotation θ in Fig. 6. V_c denotes here that part of the total shear force V which was not carried by the stirrup rein-

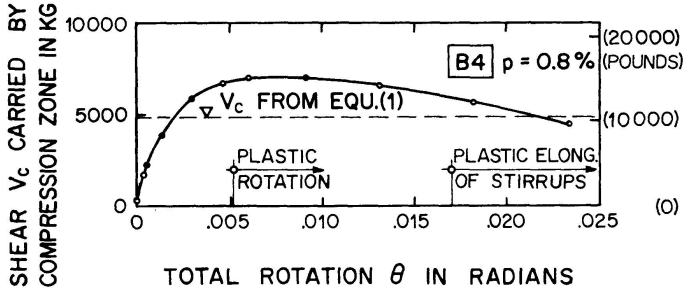

Fig. 6. Shear force V_c carried by compression zone versus total rotation θ at shear crack hinge beam B 4.

forcement according to the truss analogy; hence it was mainly carried by the concrete compression zone. In all the shear crack hinges of the described investigation a significant reduction of V_c could only be observed after some of the stirrups sustained plastic deformations. For this reason, the stress in stirrups of a shear crack hinge is essentially a function of the acting shear force. The stirrup stress does not depend primarily on the deformations produced by progressive rotation.

Further details of the test results are given in a earlier report [4].

Theoretical Investigation

The following approaches try to describe the behaviour of reinforced concrete plastic hinges by means of models which are chosen as close to reality as possible.

Flexural Crack Hinges

The model of a flexural crack hinge is shown in Fig. 7. The spacing of cracks measured along the tension reinforcement is denoted by z. All the

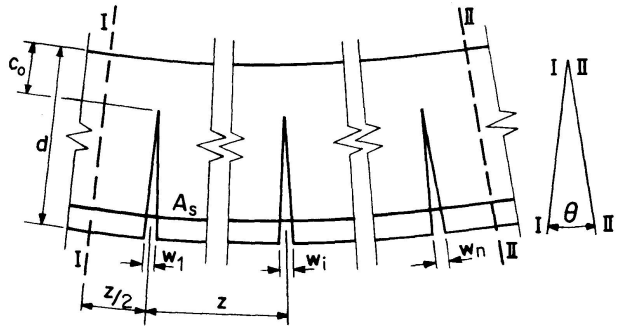

Fig. 7. Model of the flexural crack hinge.

cracks belong to the hinge in which plastic deformations of the steel occured. Neglecting the unimportant elongation of the concrete between the cracks the total rotation θ is given by Eq. (5):

$$\theta = \sum_{i=1}^{n} \frac{w_i}{d - c_0} = \frac{1}{d - c_0} \sum_{i=1}^{n} w_i . \tag{5}$$

w is the width of the crack at the level of the tensile reinforcement.

A "flexural crack element" is shown in Fig. 8. First we assume that this element is affected only by a bending moment M. For this assumption the variation of the following quantities is plotted along the tensile reinforcement:

— The steel strain ϵ_s.
— The steel stress f_s.
— The nominal bond stress u between the surface of reinforcement and the concrete.
— The slip s between the reinforcement surface and the concrete.

To calculate the values of these variables the following fundamental relationships are needed:

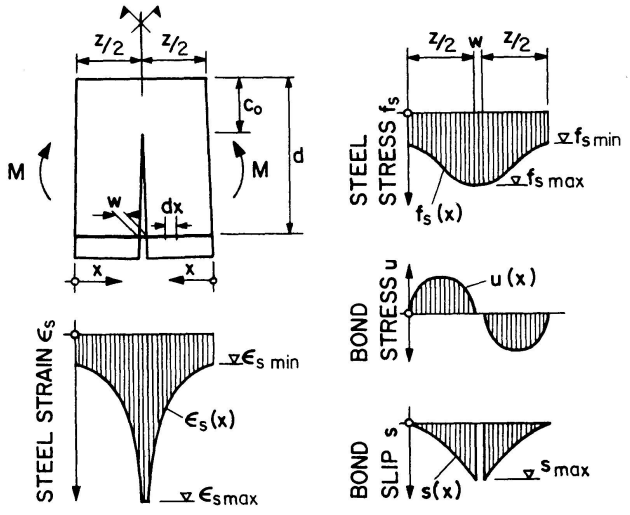

Fig. 8. "Flexural crack element" with variation of several variables.

— The bond-slip curve $u(s)$.
— The stress-strain curve $\epsilon_s(f_s)$ of the steel.

The bond-slip curve of the bar element dx can be found experimentally as shown in [5]. Typical curves for vertically embedded bars are given in Fig. 9. The bond stresses u of horizontally embedded bars are much smaller in most cases.

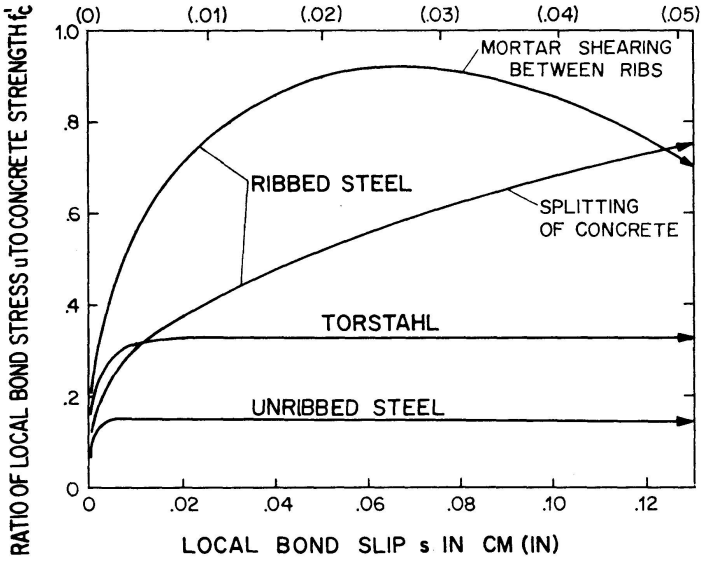

Fig. 9. Typical bond-slip curves of finite elements of vertically embedded bars.

The following relationships between the variables listed above are applic able:

$$df_s \frac{\pi D^2}{4} = u(s)\, D\, \pi\, dx; \qquad \frac{df_s}{dx} = \frac{4}{D} u(s), \tag{6}$$

$$ds = \epsilon_s(x)\, dx; \qquad \frac{ds}{dx} = \epsilon_s(f_s). \tag{7}$$

D is the diameter of the tension steel bars. A general solution of the problem for any functions $u(s)$ and $\epsilon_s(f_s)$ is given in [6]. This approach only investigates the case of steel rupture. The bond-slip curve of "Torstahl" used in the test beams is assumed to be a straight line parallel to the abscissa, hence $u(s) =$ constant $= u^*$ (compare with Fig. 9). For that reason, the function $\epsilon_s(x)$ is a part of the stress-strain curve of the steel. The Eqs. (6) and (7), respectively, lead to the following expressions for the length $z/2$ from the centre of a crack:

$$\Delta f_s = f_{s\,max} - f_{s\,min} = u^* \frac{4}{D} \frac{z}{2}, \tag{8}$$

$$s_{max} = \int_0^{z/2} \epsilon_s(x)\, dx = \frac{D}{4\, u^*} \int_{f_{s\,min}}^{f_{s\,max}} \epsilon_s(f_s)\, df_s. \tag{9}$$

If $f_{s\,max}$ and $\epsilon_{s\,max}$ are given and Δf_s is calculated from (8), the integral expression of (9) can be evaluated from the stress-strain curve of the steel.

The width of the crack is given by

$$w = 2 s_{max} (1 + \epsilon_{s\,max}). \tag{10}$$

The relationship of the average steel strain ϵ_{sa} within the flexural crack element to the maximum steel strain $\epsilon_{s\,max}$ in the crack is characterized by the bond factor κ:

$$\kappa = \frac{\epsilon_{sa}}{\epsilon_{s\,max}} = \frac{2 (1 + \epsilon_{s\,max}) \int_0^{z/2} \epsilon_s (x)\, dx}{z\, \epsilon_{s\,max}}. \tag{11}$$

The value of κ varies from 0.10 to 1.0. κ depends on $\epsilon_{s\,max}$, the shape of the stress-strain curve of the steel (especially the strain-hardening characteristic) and on the quality of the bond.

If the rupture of the steel occurs in a certain flexural crack element, No 1 say, $\epsilon_{s\,max}$ is given by Eq. (4). Then the steel stress in the crack of the neighbour element No 2 is computed by

$$f^2_{s\,max} = f^1_{s\,max} - \frac{\Delta M^{1,2}}{(d - a/2)\, A_s}, \tag{12}$$

where $\Delta M^{1,2}$ is the moment difference between the crack cross sections No 1 and No 2 of the beam at failure, a the depth of the equivalent rectangular stress block in the compression zone, and A_s is the area of the tensile steel. If M varies linearly, Eq. (12) becomes:

$$f^2_{s\,max} = f^1_{s\,max} - \frac{V z}{(d - a/2)\, A_s}. \tag{13}$$

Computing the total ultimate rotation of the hinge θ_u from Eq. (5), each flexural crack element in which plastic steel deformations are present must be taken in account.

This method neglects that the points of zero slip, $s = 0$, is not exactly midway between two adjacent cracks. This point is located slightly closer to the crack with the smaller strain $\epsilon_{s\,max}$. However, as shown in [6], the resulting error is not significant and can be neglected.

The theoretical ultimate rotations θ_{ut} of the gauge length of 25 cm (nom. 10 in.) of the test beams A 1, A 2 and A 3 were computed with this method of calculation using the material properties and the observed crack spacing of the test beams and listed in Table 1. The constant bond stress u^* was assumed to be 50 kg/cm² (nom. 700 psi). To determine ΔM, the theoretical ultimate moment distribution according to the simple plastic analysis was used, and not the measured values.

The comparison of θ_u and θ_{ut} in Table 1 shows that the measured values are 35 to 84 percent greater than the theoretical values. The value of θ_{ut} is

always on the safe side, because several effects not introduced in the theory increase the ultimate rotation. For instance the bond between the steel bars and the concrete at the border of the cracks may become loose over a certain length producing a steel strain $\epsilon_{e\,max}$ on both sides of the cracks. For this reason, it can be concluded that the developed method alwasy gives safe values of the ultimate rotation.

Considering the influence of the important variables, the ultimate rotations θ_u and θ_{ut} as determined by the rupture of the steel are found to decrease with:

— Better bond properties.
— Smaller bar diameters.
— Less strain-hardening.
— Smaller permanent steel strain.
— Greater crack spacing.
— Greater shear force.

Comparing the values of θ_{ut} listed in Table 1 with respect to the shear force it is found that the method of calculation correctly takes into account the influence of the shear force.

Shear Crack Hinges

It was found that in shear crack hinges the rotational capacity is mostly much greater than calculated by the usual methods. It will be shown here why plastic deformations can occur over a wide zone.

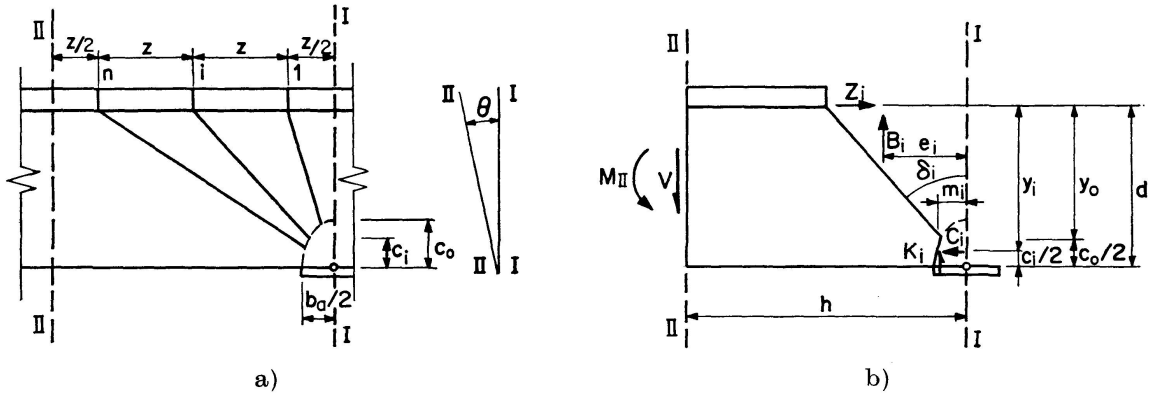

a) b)

Fig. 10. Model and internal forces of a shear crack hinge.

The model of a shear crack hinge is shown in Fig. 10a. This model corresponds to the often observed crack pattern shown in Fig. 4. The maximum inclination of the flexural-shear cracks of the hinge is characterised by tan $\delta_n = 1.3$. It is assumed that the tensile reinforcement has good bond properties (ribbed steel bars). Furthermore it is supposed that the shear reinforcement only consists of closely spaced vertical stirrups.

The part of the beam on the left of the flexural-shear crack i of Fig. 10a is shown in Fig. 10b. All the free body forces are shown. It is assumed that no

external loads exist between the cross sections I and II. Cross section II is affected by the bending moment M_{II} and the shear force V. The force in the tensile steel is denoted by Z_i. B_i is the resultant of the stirrup forces crossing the flexural-shear crack i on the left of the support. C_i and K_i denote the forces acting in the flexural compression zone parallel and perpendicular respectively to the beam axis. Any possible fixed end moment between two neighbouring cracks and dowel action of the tensile reinforcement are neglected. Furthermore, due to the large cracks widths, the shear transfer across cracks by the interlocking of aggregate particles must not be considered. The positions of the lines of action of the forces are shown in Fig. 10 also. As a simplification the distance of C_i from the extreme compression fiber is taken as $c_i/2$. c is the distance from the extreme compression fibre to the end of a flexural-shear crack (elliptical form), and b_a the support width.

With $M_I = M_{II} + V h$ the force Z_i in the tensile reinforcement is given by equilibrium conditions:

$$Z_i = \frac{M_I}{Y_i} - B_i \frac{e_i}{y_i} - K_i \frac{m_i}{y_i}. \tag{14}$$

With some transformations Eq. (14) becomes more appropriate for plotting and discussion in the following form:

$$Z_i = V \left[\frac{M_I}{V y_i} - \frac{B_i}{V} \left(\frac{e_i}{y_i} - \frac{m_i}{y_i} \right) - \frac{m_i}{y_i} \right]. \tag{15}$$

B_i/V can be expressed for $\tan \delta_i \geqq b_a/2$ as follows:

$$\frac{B_i}{V} = \frac{B_{45}}{V} \left[\frac{\tan \delta_i - b_a/2d}{1 - b_a/2d} \right]. \tag{16}$$

B_{45} is the resultant of the stirrup forces crossing a 45° crack. Furthermore, if c_0/d and b_a/d are given, the distances e_i, m_i, and y_i are a function of the angle δ_i alone. When using Eq. (16) care must be taken that the condition $B_i/V \geqq 1.0$ is always satisfied.

For flexural cracks perpendicular to the beam axis instead of inclined flexural-shear cracks, the tensile force Z_i would be given by

$$Z_i = V \left[\frac{M_I}{V y_0} - \frac{d}{y_0} \tan \delta_i \right]. \tag{17}$$

In this formula $\tan \delta_i$ characterises the distance from the considered flexural crack to the point of maximum moment (cross section I). Eq. (17) also gives the tensile force corresponding to the usual bending theory of reinforced concrete beams with y_0 as the lever arm of the internal bending forces: $Z_i = M_i/y_0$.

When discussing the derived formulas the following values are usually assumed:

$$\frac{c_0}{d} = 0.2; \qquad \frac{b_a}{d} = 0.3.$$

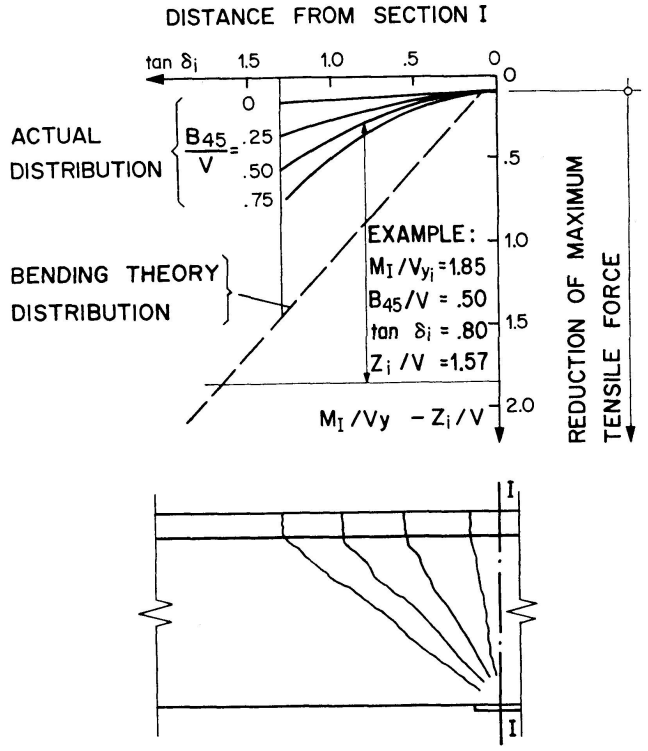

Fig. 11. Distribution of the tensile force in a shear crack hinge.

A dimensionless diagram of the distribution of the tensile force for several assumptions is given in Fig. 11. On the abscissa the distance from the cross section under consideration to cross section I is characterised by tan δ_i. On the ordinate the values of $(M_I/V\,y - Z_i/V)$, which are calculated by Eqs. (15) and (17) are plotted. Therefore, the ordinate values correspond to the reduction of the maximum amount of the tensile force over the support.

For several values of the ratio B_{45}/V the actual force distribution in a zone of flexural-shear cracks is given in the upper part of Fig. 11. B_{45}/V characterises the stress and efficiency of the shear reinforcement. The portion K_{45} of the shear force V which is not transferred by the shear reinforcement is carried by the compression zone. Since the values of M_{45} are always greater than or equal to $V_C = v_c b' d$, the value of B_{45}/V essentially depends on the shear force $V = v b' d$. As a result, B_{45}/V is often very low. But if a very high shear stress v exists, B_{45}/V increases to a maximum value of about 0.75. Furthermore, the distribution of the tensile force, assuming flexural cracks or calculated by the usual bending theory, is shown in Fig. 11. The tensile force is proportional to the bending moment.

In Fig. 11 it can be seen that in a zone of flexural-shear cracks the reduction of the maximum tensile force is relatively low. This explains the wide spread of plastic deformations in shear crack hinges. Since the small force reduction can be compensated by strain hardening of the steel the plastic length of the hinge on both sides of the support often is equal to or greater than the effective depth of the beam.

Dependence of Rotational Capacity on Shear Stress

The dependence of the ultimate rotation θ_u on the shear stress v is shown only generally and qualitatively in Fig. 12. If $v < v_k$ flexural cracks only occur. If $v > v_k$ flexural-shear cracks are developed. Corresponding to these crack

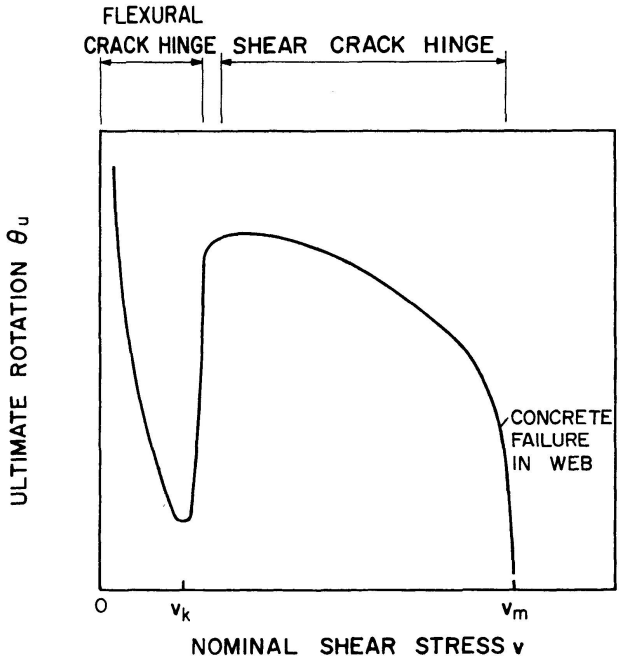

Fig. 12. General dependence of ultimate rotation θ_u on the nominal shear stress v.

patterns a flexural crack hinge or a shear crack hinge develops. In a flexural crack hinge the plastic deformations are concentrated into a smaller zone the greater v is. The value of the ultimate rotation θ_u accordingly decreases. Assuming that a rupture of the steel occurs, the reduction of θ_u is very high. In the case of a concrete fracture a reduction is also confirmed. If the shear stress is enough to produce flexural-shear cracks, the rotation θ_u considerably increases since plastic deformations occur on a much wider zone. With increasing shear stress v the ultimate rotation θ_u decreases again. But if sufficient shear reinforcement exists, a drastic reduction of θ_u only occurs as $v \to v_m$ through crushing of the concrete in the web due to shearing deformations and inclined compression forces. Depending on several conditions the values of v_k and v_m can vary considerably. From tests it can be concluded that v_k and v_m reach approximately the value of v_c and $(4-5)\,v_c$, respectively.

Conclusions

As a result of this experimental and theoretical investigation the following conclusions can be made:

1. According to the amount of shear stress two quite different types of plastic hinges are produced:

— "Flexural crack hinges" which occur in the beam zone mainly affected by a bending moment, and only producing flexural cracks perpendicular to the beam axis (Fig. 3), and

— "Shear crack hinges" which occur in the beam zones which are, in addition to a bending moment, affected by a considerable shear force, and exhibit inclined flexure-shear cracks (Fig. 4).

2. In a flexural crack hinge plastic deformations may be concentrated to a single or only a few flexural cracks. For this reason the rotational capacity may be very small.

3. The danger of a steel rupture can follow from good bond properties of the tensile reinforcement in a flexural crack hinge, since the steel strain only increases in the cracks, while between the cracks the steel strain is still in the elastic range.

4. The usual method of calculating the rotational capacity by integrating a "curvature of rupture" over a "plastic length" may lead to severe errors. The values of ultimate rotation in the case of a steel rupture measured in the described tests reach only 20 to 59 percent of the values calculated by the usual method mentioned above.

5. Therefore, the rotational capacity of flexural crack hinges, particularly in case of a steel rupture, should be investigated with the corresponding crack model (Fig. 7). This method correctly takes into account the influence of bond, bar diameter, strain and strain-hardening properties of tensile reinforcement, as well as the influence of shear force. Thus, this theory gives safe lower limit values of the ultimate rotation.

6. On the other hand plastic deformations in shear crack hinges usually extend over a relatively wide zone. For this reason, the rotational capacity is correspondingly high.

7. This observation can be explained with the aid of the crack model for the shear crack hinge (Fig. 10). The tensile force in the steel is considerably greater than in the case of flexural cracks only or calculated by the usual bending theory.

8. In shear crack hinges the stress of vertical stirrups is mainly a function of the value of the shear force. The stirrup forces do not depend on the deformations in the hinge caused by progressive rotation.

9. In a zone of flexural cracks the shear stress may considerably decrease the rotational capacity. However, if the shear stress is high enough to produce inclined flexural-shear cracks, the rotational capacity is significantly increased.

Notation

A_s area of tensile reinforcement
a depth of the equivalent rectangular stress block in compression zone
B resultant of stirrup forces crossing a flexure-shear crack
b width of compression face
b' width of web
b_a support width
C compression force in bending compression zone
c distance from extreme compression fibre to the end of a flexure-shear crack
c_0 distance from extreme compression fibre to neutral axis and to the end of flexural crack
D bar diameter
d distance from extreme compression fibre to centroid of tensile reinforcement
E_s modulus of elasticity of steel
e distance of the line of action of B from the support in a shear crack hinge
f'_c compressive strength of concrete
f_e elastic limit stress of reinforcement (0.005 percent proof stress)
f_s tensile stress in steel
f'_s tensile strength of reinforcement
f_y yield strength of reinforcement (0.2 percent proof stress)
h distance of the line of action of V from the support in a shear crack hinge
K shear force in bending compression zone of a shear crack hinge
L_p plastic length of hinge
M bending moment
M_u ultimate bending moment
m distance fixing the acting line of K in a shear crack hinge
p tensile steel ratio A/bd
s slip between reinforcement surface and concrete
u nominal bond stress between reinforcement surface and concrete
V shearing force
V_c shear force carried by the concrete compression zone
V_u shear force at ultimate moment
v nominal shear stress $v = V/b'd$
v_u nominal shear stress at (ultimate moment) M_u
v_k nominal shear stress at which flexure-shear cracks are developed
v_m nominal shear stress at failure due to crushing of the concrete
v_c nominal shear stress in concrete compression zone
w width of a crack at tensile reinforcement
y distance determining the line of action of Z in a shear crack hinge
Z force in tensile reinforcement
z spacing of cracks measured along tensile reinforcement

δ angle between a flexure-shear crack and a line perpendicular to the beam axis
ϵ_{cu} maximum concrete compressive strain at M_u
ϵ_s tensile strain in steel
ϵ_{sa} average steel strain
ϵ_{su} permanent steel elongation as a percentage measured on test bars outside of rupture
θ total rotation occurring within the plastic length L_p
θ_u total rotation at ultimate moment M_u
θ_{uc} total rotation calculated by the method as given in [2] and [3] (failure due to failure of concrete)
θ_{us} total rotation calculated by Eq. (3) (failure due to rupture of steel)
λ ratio of calculated ultimate moment in span and over the central support

Acknowledgement

The beam tests were made possible by a research grant from the Von Moossche Eisenwerke at Lucerne (Switzerland) which is gratefully acknowledged. Furthermore the author wishes to thank Prof. Dr. B. Thürlimann and Prof. E. Amstutz from the Swiss Federal Institute of Technology (ETH), Zurich, under whose guidance and with whose help this research programme has been carried out.

References

[1] B. Thürlimann, H. Ziegler: Plastische Berechnungsmethoden (Plastic Design Method). Autographie der Vorlesungen vom Fortbildungskurs für Bau- und Maschineningenieure, ETH, Zürich, 1963.

[2] ACI-ASCE Committee 428: Progress Report on Code Clauses for Limit Design. ACI Journal, Proceedings V. 65, No. 9, September 1968, p. 713–720.

[3] W. G. Corley: Rotational Capacity of Reinforced Concrete Beams. Proceedings, ASCE, V. 92, No. ST 5, October 1966, p. 121–146; also PCA Development Bulletin D-108.

[4] H. Bachmann, B. Thürlimann: Versuche über das plastische Verhalten von zweifeldrigen Stahlbetonbalken (Tests on the Plastic Behavior of Two-Span Reinforced Concrete Beams). Berichte Nr. 6203-1 und 6203-2 des Instituts für Baustatik an der Eidgenössischen Technischen Hochschule (ETH), Zürich, 1965.

[5] G. Rehm: Über die Grundlagen des Verbundes zwischen Stahl und Beton (On the Bond between Steel and Concrete). Deutscher Ausschuß für Stahlbeton, Heft Nr. 136, Berlin 1961.

[6] H. Bachmann: Zur plastizitätstheoretischen Berechnung statisch unbestimmter Stahlbetonbalken (On the Plastic Design of Statically Indeterminate Reinforced Concrete Beams). Bericht Nr. 13 des Instituts für Baustatik an der Eidgenössischen Technischen Hochschule (ETH), Zürich, Juli 1967.

Summary

10 two-span reinforced concrete beams were tested to study the influence of shear and bond on the rotational capacity of reinforced concrete plastic hinges.

The shear stress determines whether a "flexural crack hinge" or a "shear crack hinge" occurs. In flexural crack hinges the rotational capacity can be considered smaller than the values calculated by usual methods. Therefore a new method of calculation giving safe values has been developed. On the other hand in shear crack hinges plastic deformations occur within a wide zone allowing a larger rotational capacity.

Résumé

On a fait des essais avec dix poutres en béton armé à deux travées pour étudier l'influence de la sollicitation de cisaillement et de l'adhérence des armatures sur la capacité de rotation des rotules plastiques en béton armé.

Suivant la valeur de la sollicitation de cisaillement, il résulte une „rotule due à une fissure de flexion" ou une „rotule due à une fissure de cisaillement". Dans des rotules dues à la flexion, la capacité de rotation peut être très inférieure à celle calculée d'après les méthodes usuelles. Par conséquent, il est nécessaire de développer une nouvelle méthode de calcul qui donne des résultats sûrs. Au contraire, dans des rotules dues au cisaillement, les déformations qui s'étendent sur un large domaine provoquent une grande capacité de rotation.

Zusammenfassung

Es wurden Versuche an 10 zweifeldrigen Stahlbetonbalken gemacht zwecks Studium des Einflusses von Schubbeanspruchung und Verbund auf die Rotationsfähigkeit plastischer Stahlbeton-Gelenke.

Je nach Höhe der Schubbeanspruchung entsteht ein „Biegeriß-Gelenk" oder ein „Schubriß-Gelenk". In Biegeriß-Gelenken kann die Rotationsfähigkeit wesentlich kleiner sein als sie sich nach üblichen Methoden berechnen läßt. Daher wird eine neuartige Berechnungsmethode entwickelt, die sichere Resultate liefert. Demgegenüber entstehen in Schubriß-Gelenken plastische Verformungen über einen weiten Bereich, die eine entsprechend große Rotationsfähigkeit bewirken.